COMPUTATION OF HOLLOW CYLINDER EXPLOSIONS

Aivars Celmins

Ballastic Research Laboratories
Aberdeen Proving Ground, Maryland

November 1967

BRL R 1381

BRL

AD

REPORT NO. 1381

COMPUTATION OF HOLLOW CYLINDER EXPLOSIONS

by

Aivars Celmiņš

November 1967

U. S. ARMY MATERIEL COMMAND
BALLISTIC RESEARCH LABORATORIES
ABERDEEN PROVING GROUND, MARYLAND

Destroy this report when it is no longer needed.
Do not return it to the originator.

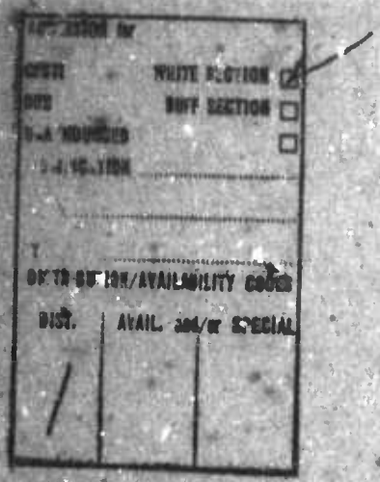

The findings in this report are not to be construed as an official Department of the Army position, unless so designated by other authorized documents.

B A L L I S T I C R E S E A R C H L A B O R A T O R I E S

REPORT NO. 1381

NOVEMBER 1967

COMPUTATION OF HOLLOW CYLINDER EXPLOSIONS

Aivars Celmiņš

Computing Laboratory

This material was presented at the 13th Conference of Army Mathematicians, Fort Monmouth, New Jersey on June 7-8, 1967.

RDT&E Project No. 1T014501A14B

A B E R D E E N P R O V I N G G R O U N D, M A R Y L A N D

B A L L I S T I C R E S E A R C H L A B O R A T O R I E S

REPORT NO. 1381

ACelmiņš/bj/sjw
Aberdeen Proving Ground, Md.
November 1967

COMPUTATION OF HOLLOW CYLINDER EXPLOSIONS

ABSTRACT

This report treats the explosion caused by a charge which is placed between two hollow co-axial cylinders. It is assumed that at the beginning of the motion of the cylinders the explosive has been detonated completely so that the space between the cylinders is filled by a gas under high pressure. The flow of this gas during the collapse of the inner cylinder and the expansion of the outer cylinder is governed by a quasi-linear second order partial differential equation. This equation is solved numerically using a two-level difference scheme. The solution furnishes the fragment velocities of the outer cylinder and the collapse velocity of the inner cylinder. The results are compared with experimental data and asymptotic formulae.

The same computation scheme is applied to the computation of the motions of two parallel plates with a charge exploded between them. The results agree with values obtained by approximate formulae.

TABLE OF CONTENTS

INTRODUCTION

Fragment velocities of exploded cylinders have been investigated in the past mainly by experiment. In addition to experimental results some approximate formulae for the velocities have been established by Gurney and Sterne using energy considerations.[3,8*] In general these formulae provide, together with adequate experiments, satisfactory results. However, if the explosive is located between two co-axial hollow cylinders, no such formula can be derived by the method used by Gurney and Sterne. In such cases one must rely only on experiments which may furnish the velocities of fragments of the outer cylinder. The measurement of the collapse velocity of the inner cylinder apparently requires more complicated techniques and no publications of such measurements are known to the author. On the other hand, the knowledge of the collapse velocity can be of some help for studies of shaped charge problems.

One possible method to compute the collapse process of the inner cylinder is treated in this paper. We arrive at this method by formulating first an equation of motion for the flow of explosive fumes in the space between the two cylinders. Boundary conditions for this equation are established by considering the properties of the cylinders. The solution of this equation furnishes then the desired collapse and fragment velocities.

The equation of motion formulated and treated here is a quasi-linear second order partial differential equation. It is solved numerically by using a two-level difference scheme.

---

*Superscript numbers denote references which may be found on page 50.

Only some of the results obtained by the numerical integration of the differential equation can be compared with experimental data, namely the positions of the fragments of the outer cylinder at given instants. This comparison shows that the computations are compatible with experiments. A close agreement is obtained during the early phase of the explosion.

In special cases the numerical solution can be compared with the approximate formulae mentioned above. In all cases where such formulae exist both results agree completely. An equally close agreement of results was obtained for the case in which the cylinders are degenerated into parallel plates. These agreements indicate that the numerical solution process employed is sufficiently accurate.

Disagreements between experimental results and numerical solutions may be caused by inadequate assumptions made for the development of the theory. These assumptions can be changed and the theory correspondingly refined when more accurate experimental data are available. The theory developed permits such refinement.

CHAPTER 1
PROBLEM OUTLINE

Assume that the space between two co-axial metal cylinders is filled with an explosive. The detonation of the explosive may cause the outer cylinder to burst and the inner cylinder to collapse. We are primarily interested in the motion of the inner cylinder after such a detonation. We obtain a similar problem if we replace the cylinders by two parallel plates with the explosive located between the plates. Mathematically this problem is a limit case of the first one if we let the radii of the cylinders become infinite.

The gas flow and mass motions during the process described depend in a rather complicated manner on a large number of parameters. In order to reduce the number of parameters we will treat a simplified model of the processes. This model is obtained by assuming the following idealizations of the real problem.

1. The cylinders are infinitely long and all motions are circular symmetric and identical for all orthogonal cross-sections of the cylinders. This assumption reduces the problem to that of a one-dimensional flow which is cylindrical for finite radii of the cylinders.

2. The explosive is detonated completely before the cylinders start moving. This assumption means that the space between the cylinders is filled with a high pressure gas at the beginning of the motion of the cylinders.

3. The gas between the cylinders is a perfect inviscid gas and the gas flow is adiabatic, i.e., without heat exchange between gas particles. This assumption may be justified by the observation that we are interested in the first phase of the motion only, that is until the complete compression of the liner. The flow during this phase resembles very much a simple wave. Particularly we can expect that no shocks will develop in the flow during this phase, the duration of which might be some 10^{-5} seconds.

4. The outer cylinder is surrounded by vacuum, and vacuum is also inside the inner cylinder. This assumption specifies the type of the boundary conditions for the gas flow. A complete formulation of the boundary conditions requires more detailed assumptions about the cylinders. These assumptions will be discussed in separate chapters treating the boundary conditions.

CHAPTER 2
EQUATION OF MOTION

For the description of the problem we use cylindrical coordinates r, φ, z (Figure 2.1). The position of a gas particle which was originally at the distance R from the cylinder axis is independent of the coordinates φ and z because of the Assumption 1. Hence the status of the system is completely described by the distance r of any gas particle from the axis. Our system is thus one-parametric and can be described by the function r(R,t) with the property

$$r(R,0) = R. \tag{2.1}$$

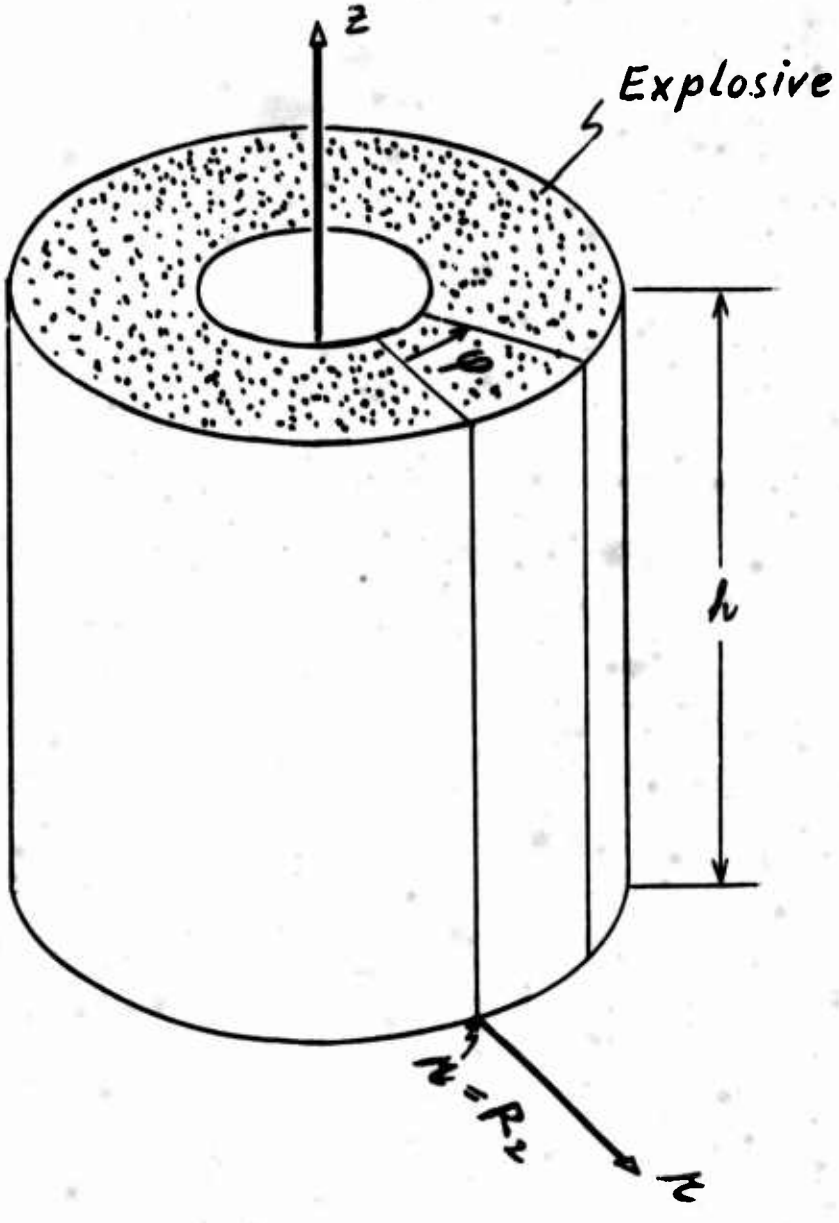

Figure 2.1

In this Chapter we will derive a differential equation for the function r(R,t). To this end we consider first the forces acting on a volume element V of the gas. At time t = 0 the element may have the coordinate R and its volume is (Figure 2.2)

$$V(R,0) = R.dR\ h\varphi + \tfrac{1}{2}(dR)^2\ h\varphi \qquad (2.2)$$

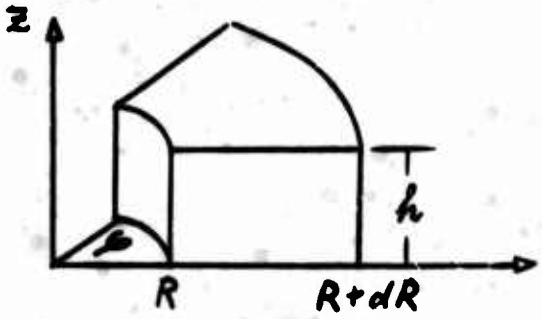

Figure 2.2

At time t the gas which was originally in V(R,0) has moved to r(R,t) and it occupies the volume (Figure 2.3)

$$V(R,t) = r\frac{\partial r}{\partial R}\,dR\cdot h\cdot\varphi + 0(\varphi\cdot(dR)^2) \qquad (2.3)$$

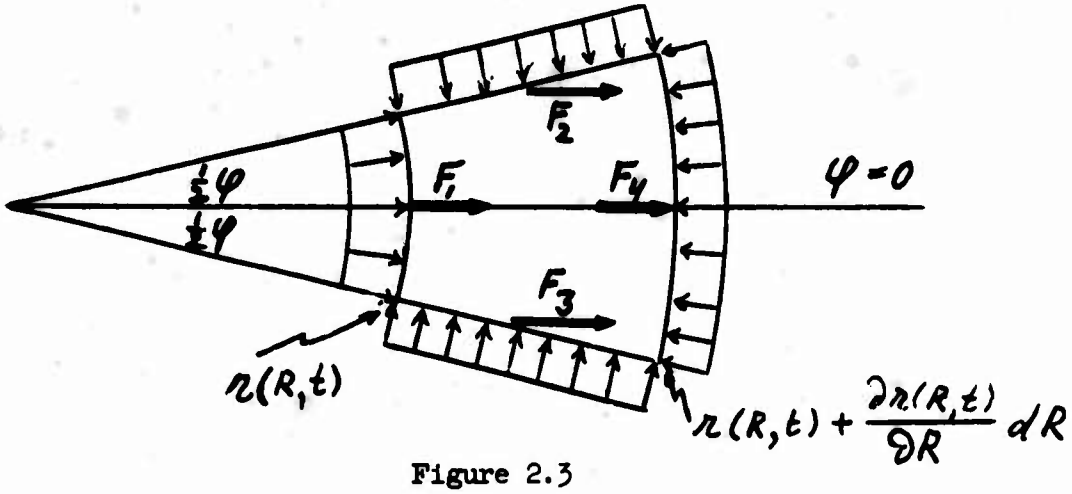

Figure 2.3

The forces acting on the element are caused by the pressure p(R,t) within the gas. Because of the circular symmetry assumed we need to consider the resultants of the pressure in the direction φ = 0 of Figure 2.3

only. (Other components cancel each other.) These resultants are

$$F_1 = p.r.h.2.\sin \tfrac{1}{2}\varphi$$

$$F_2 = F_3 = p\frac{\partial r}{\partial R}.dR.h.\sin \tfrac{1}{2}\varphi + \sin \tfrac{1}{2}\varphi\, O((dR)^2)$$

$$F_4 = -(p.r + p\frac{\partial r}{\partial R}dR + r\frac{\partial p}{\partial R}dR)\, h.2 \sin \tfrac{1}{2}\varphi + O((dR)^2 \sin \tfrac{1}{2}\varphi)$$

The sum of these forces is

$$F = -\frac{\partial p}{\partial R}.r.dR.h.2 \sin \tfrac{1}{2}\varphi + O((dR)^2 \sin \tfrac{1}{2}\varphi). \qquad (2.4)$$

With $\rho(R,t)$ being the density of the gas at $r(R,t)$, we obtain from (2.3) and (2.4)

$$\frac{\partial^2 r}{\partial t^2}.\rho r\frac{\partial r}{\partial R} = -\frac{\partial p}{\partial R}.r.\frac{2 \sin \tfrac{1}{2}\varphi}{\varphi} + O(dR). \qquad (2.5)$$

For $dR \to 0$ and $\varphi \to 0$ the last equation becomes

$$\frac{\partial^2 r}{\partial t^2} \cdot \rho\frac{\partial r}{\partial R} r = -\frac{\partial p}{\partial R}.r. \qquad (2.6)$$

A second equation we obtain by considering the mass within the volume element V. Since in our system no new mass is created, the quantity ρV must remain constant. We conclude, therefore, from (2.2) and (2.3)

$$\rho r\frac{\partial r}{\partial R} = \rho(R,0).R + O(dR)$$

or, with $dR \to 0$

$$\rho r\frac{\partial r}{\partial R} = \rho(R,0).R. \qquad (2.7)$$

Substitution of (2.7) into (2.6) yields

$$\frac{\partial^2 r}{\partial t^2} = - \frac{1}{\rho(R,0)} \frac{r}{R} \cdot \frac{\partial p}{\partial R} \,. \tag{2.8}$$

The initial density distribution $\rho(R,0)$ we may consider as known. However, the Equation (2.8) still contains the unknown quantity $\partial p/\partial R$. In order to eliminate this quantity we have to make some assumptions about the properties of the gas. (So far we have only assumed that the gas is inviscid in the derivation of Equation (2.6)). Here we use Assumption 3 which furnishes the following relation between the pressure p and density ρ for an adiabatic flow of an inviscid perfect gas:

$$\frac{\partial}{\partial t} \left(\frac{p}{\rho^\gamma}\right) \equiv 0. \tag{2.9}$$

The exponent γ is the ratio of specific heats for the gas (Ref.1,p. 10). From (2.9) we deduce the relation

$$p(R,t) = p(R,0) \cdot \frac{\rho(R,t)^\gamma}{\rho(R,0)} \tag{2.10}$$

Substitution of (2.7) into (2.10) furnishes

$$p(R,t) = p(R,0) \cdot \left(\frac{R}{r \cdot \partial r/\partial R}\right)^\gamma. \tag{2.11}$$

With (2.11) we can eliminate the pressure from the Equation (2.8). The result is

$$\frac{\partial^2 r}{\partial t^2} = - \frac{1}{\rho(R,0)} \cdot \frac{r}{R} \cdot \frac{\partial}{\partial R} \left\{ p(R,0) \left(\frac{R}{r \cdot \partial r/\partial R}\right)^\gamma \right\} \tag{2.12}$$

or

$$\frac{\partial^2 r}{\partial t^2} = \frac{p(R,0)}{\rho(R,0)} \gamma \left(\frac{R}{r}\right)^{\gamma-1} \left(\frac{\partial r}{\partial R}\right)^{-\gamma-1} \left[\frac{\partial^2 r}{\partial R^2} + \frac{1}{r}\left(\frac{\partial r}{\partial R}\right)^2 - \frac{1}{R}\frac{\partial r}{\partial R} - \right.$$

$$\left. - \frac{1}{p(R,0)} \cdot \frac{\partial r}{\partial R} \cdot \frac{\partial p(R,0)}{\partial R}\right] . \quad (2.13)$$

This final equation of motion is a quasi-linear second order partial differential equation for the function $r(R,t)$ in case of a cylindrical flow. The functions $\rho(R,0)$ and $p(R,0)$ we consider as given initial values for the problem.

For comparison we derive the corresponding equation of motion for cylinders which have degenerated into plates. In order to carry out the limiting process we write

$$\begin{aligned} r &= \hat{r} + \tilde{R}, \\ R &= \hat{R} + \tilde{R}, \\ p(R,t) &= \hat{p}(\hat{R},t), \\ \rho(R,t) &= \hat{\rho}(\hat{R},t) \end{aligned} \quad (2.14)$$

and let $\tilde{R} \to \infty$. The limiting process applied onto (2.13) yields then the equation

$$\frac{\partial^2 \hat{r}}{\partial t^2} = \frac{\hat{p}(\hat{R},0)}{\hat{\rho}(\hat{R},0)} \gamma \left(\frac{\partial \hat{r}}{\partial \hat{R}}\right)^{-\gamma-1} \left[\frac{\partial^2 \hat{r}}{\partial \hat{R}^2} - \frac{1}{\hat{p}(\hat{R},0)} \cdot \frac{\partial \hat{r}}{\partial \hat{R}} \cdot \frac{\partial \hat{p}(\hat{R},0)}{\partial \hat{R}}\right]. \quad (2.15)$$

The most significant difference between the Equations (2.13) and (2.15) is the factor $r^{1-\gamma}$ in (2.13). As the gas flow approaches the axis of the cylinder this factor might cause an increase of the acceleration. In the equation of motion (2.15) neither the independent variable $\hat{R}$ nor the dependent variable $\hat{r}$ appears explicitly. This indicates the absence

of any effects of the geometry of the experiment onto the flow. For the flow represented by (2.15) we would, therefore, expect a gradual decrease of acceleration to zero due to the loss of pressure as the gas expands.

In order to have in the sequel a uniform formulation for cylinders and plates we will use, whenever convenient, for the independent variables R or $\hat{R}$ the symbol x (assuming $a \le x \le b$) and for the unknown functions $r(R,t)$ or $\hat{r}(\hat{R},t)$ the symbol $u(x,t)$. Then the equation of motion for cylindrical flow is

$$u_{tt} = \frac{p(x,0)}{\rho(x,0)} \cdot \gamma \cdot \left(\frac{x}{u}\right)^{\gamma-1} \frac{1}{u_x^{\gamma+1}} \left[u_{xx} + \frac{u_x^2}{u} - \frac{u_x}{x} - u_x \frac{p_x(x,0)}{p(x,0)} \right] \quad (2.16)$$

and in case of plates

$$u_{tt} = \frac{p(x,0)}{\rho(x,0)} \gamma \frac{1}{u_x^{\gamma+1}} \left[u_{xx} - u_x \frac{p_x(x,0)}{p(x,0)} \right]. \quad (2.17)$$

We see that in both cases the following three parameters determine the flow:

(1) the ratio of specific heats, γ;

(2) the function

$$P(x) = \frac{p(x,0)}{\rho(x,0)} ; \quad (2.18)$$

(3) the function

$$Q(x) = \frac{p_x(x,0)}{p(x,0)} .$$

The quantity γ is a known parameter of the explosive. The functions P(x) and Q(x) depend in a simple manner on the initial status of the gas.

CHAPTER 3
SPECIFIC PROPERTIES OF CYLINDRICAL FLOW

Investigations of centripetal cylindrical flows of incompressible liquid show very high pressures and velocities when the flow approaches the axis of the cylinder[2]. It has been anticipated that the compressibility of a real liquid would reduce the pressures and velocities (*loc. cit.*). The question arises whether such a reduction is sufficiently large to cancel completely the increase of pressure in a centripetal flow. The following investigation will demonstrate that generally such is not the case for adiabatic flows.

Assume that the flow starts at time t = 0 with the following initial values

$$\begin{aligned} r(R,0) &= R \\ \frac{\partial r(R,0)}{\partial t} &= v(R) < 0, \\ p(R,0) &= p_o(R), \\ \rho(R,0) &= \rho_o(R). \end{aligned} \tag{3.1}$$

R is, as in Chapter 2, the Lagrangian coordinate of the problem, v(R) is the particle velocity and p and ρ are the pressure and density, respectively.

By substitution of (3.1) into the equation of motion (2.9) we compute the initial values of the second time derivative:

$$\frac{\partial^2 r(R,0)}{\partial t^2} = - \frac{p_o'(R)}{\rho_o(R)} \tag{3.2}$$

For time t > 0 we obtain by expanding r(R,t), $\frac{\partial r(R,t)}{\partial R}$ and $\frac{\partial r(R,t)}{\partial t}$ in power series of t

$$r(R,t) = R + t\cdot v(R) - \frac{1}{2}\, t^2\, \frac{p_o'(R)}{\rho_o(R)} + O(t^3), \tag{3.3}$$

$$\frac{\partial r(R,t)}{\partial R} = 1 + tv'(R) - \frac{1}{2}\, t^2 \left(\frac{p_o'(R)}{\rho_o(R)}\right)' + O(t^3), \tag{3.4}$$

$$\frac{\partial r(R,t)}{\partial t} = v(R) - t\, \frac{p_o'(R)}{\rho_o(R)} + O(t^2). \tag{3.5}$$

The corresponding value of $p(t,R)$ we obtain by substituting (3.3) and (3.4) into (2.11). (The Equation (2.11) was derived under the assumption of an adiabatic flow from the condition for conservation of mass.) The result is

$$p(R,t) = p_o(R)\left\{\frac{R}{r(R,t)\cdot \partial r/\partial R}\right\}^{\gamma} =$$

$$= p_o\left\{1 + t\left(\frac{v}{R} + v'\right) + t^2\left(\frac{vv'}{R} - \frac{1}{2}\,\frac{p_o'}{\rho_o} - \frac{1}{2}\left(\frac{p_o'}{\rho_o}\right)'\right) + O(t^3)\right\}^{-\gamma} =$$

$$= p_o\left\{1 - \gamma t\left(\frac{v}{R} + v'\right) + \right. \tag{3.6}$$

$$\left. + t^2\left[\frac{\gamma(\gamma+1)}{2}\left(\frac{v}{R} + v'\right)^2 - \gamma\frac{vv'}{R} + \frac{1}{2}\,\gamma\left(\frac{p_o'}{\rho_o} + \left(\frac{p_o'}{\rho_o}\right)'\right)\right]\right\} + O(t^3).$$

The difference between the pressure at time t and the initial pressure is

$$p(R,t) - p_o(R) = -\, p_o\gamma t\left(\frac{v}{R} + v'\right) + \tag{3.7}$$

$$+ \frac{1}{2}\,\gamma\, p_o t^2\left[\gamma\left(\frac{v}{R} + v'\right)^2 + \left(\frac{v}{R} - v'\right)^2 + \frac{p_o'}{\rho_o} + \left(\frac{p_o'}{\rho_o}\right)'\right] + O(t^3).$$

From (3.7) we conclude that the pressure in the flow will increase whenever

$$R\, v'(R) < -\, v(R). \tag{3.8}$$

For a centripetal flow $v(R) < 0$. Therefore, (3.8) can be satisfied for any $v'(R)$ if R is sufficiently small. Hence we can conclude than an increase of pressure in a centripetal flow is possible even if $v'(R) > 0$, i.e., for flows where the particles nearer to the axis have higher velocities.

In the special case $v(R) = \text{const.}$ the pressure will increase throughout the flow, i.e., for all values of R.

We consider now another special case, namely $p_o(R) = \text{const.}$ and ask whether the pressure gradient can become negative when the pressure has increased. First we note that for $p_o(R) = \text{const.}$ the second term in (3.7) is positive and, therefore, (3.8) is sufficient to insure an increase of pressure up to third order terms in t.

The gradient of the pressure $p(R,t)$ is in the case considered

$$\frac{\partial p(R,t)}{\partial R} = -\, p_o \gamma t\left(\frac{v}{R} + v'\right)' + p_o \gamma^2 t^2 \left(\frac{v}{R} + v'\right)\left(\frac{v}{R} + v'\right)' + \tag{3.9}$$

$$+\, p_o \gamma t^2 \left(\frac{v}{R} - v'\right)\left(\frac{v}{R} - v'\right)' + O(t^3)$$

For small t this gradient is negative if

$$D[v] = v'' + \frac{v'}{R} - \frac{v}{R^2} > 0 \tag{3.10}$$

and any negative function $v(R)$ which satisfies (3.8) and (3.10) will cause an increase of the pressure and a negative pressure gradient. The simplest example of such a function is

$$v(r) = C_1 + C_2 R. \tag{3.11}$$

This function satisfies (3.8) if

$$(\frac{v}{R} + v') \cdot R = C_1 + 2C_2 R < 0 \qquad (3.12)$$

and it satisfies (3.10) if

$$(\frac{v}{R} - v')R = C_1 < 0. \qquad (3.13)$$

Clearly, if (3.12) and (3.13) are both satisfied the function $v(R) < 0$. Furthermore, this function makes the second term in (3.9) negative and the third term equal to zero. Therefore, positive terms in the expression (3.9) for the gradient of the pressure are at least of third order in t.

Figure 3.1 shows such linear velocity profiles v(R) over the Lagrangian coordinate R which satisfy the conditions for increasing pressure and negative pressure gradient.

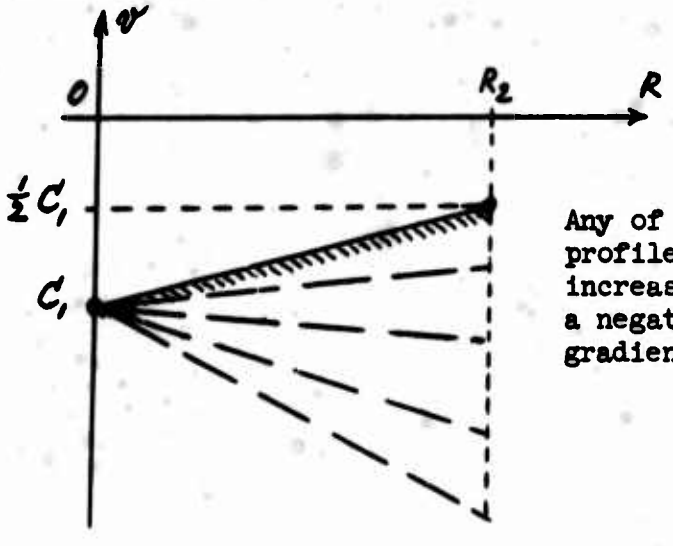

Figure 3.1

For comparison we carry out the same analysis as above for cylinders degenerated into plates. Because the condition for the conservation of mass is now different we obtain instead of (3.6) the following equation for the pressure:

$$p(R,t) = p_o(R)\left\{\frac{1}{\partial r/\partial R}\right\}^{\gamma} =$$

$$= p_o(R)\left\{1 + tv'(R) - \frac{1}{2}t^2\left(\frac{p_o'}{\rho_o}\right)' + O(t^3)\right\}^{-\gamma} = \tag{3.14}$$

$$= p_o(R)\left\{1 - \gamma\, t\, v'(R) + \right.$$

$$\left. + \frac{1}{2}t^2\left[\gamma(\gamma+1)v'^2 - \gamma\left(\frac{p_o'}{\rho_o}\right)'\right]\right\} + O(t^3).$$

As a condition for the increase of pressure we obtain instead of (3.8) simply

$$v'(R) < 0. \tag{3.15}$$

The pressure gradient of an initially constant pressure becomes now

$$\frac{\partial p(R,t)}{\partial R} = -\gamma\, t\, v'' + t^2\gamma(\gamma+1)v'v'' + O(t^3). \tag{3.16}$$

A negative gradient of the increased pressure will therefore be obtained if v(R) satisfies in addition to (3.15) the condition

$$v''(R) > 0. \tag{3.17}$$

As in the case of a cylindrical flow both conditions together insure the increase of pressure and negative gradient up to terms of third order in t.

Figure 3.2 shows a typical velocity profile satisfying (3.15) and (3.17). The main differences between the profiles shown in Figures 3.1

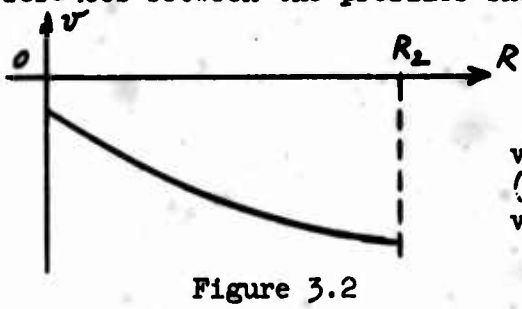

v(R) satisfies in (0,R) the conditions $v' < 0$ and $v'' > 0$.

Figure 3.2

and 3.2 is that the pressure in a cylindrical centripetal flow increases not only in all such cases where it would increase in a linear flow but also in other cases with positive velocity gradient. (Condition (3.15) implies (3.8) because $v < 0$.) Therefore, pressure increase in a cylindrical centripetal adiabatic flow is possible and, if the velocity gradient remains finite, likely for small R. The maximum pressures obtained in such flows depend on the boundary conditions which have not been discussed in this analysis.

CHAPTER 4
BOUNDARY CONDITIONS FOR THE CASING

Boundary conditions for the gas flow at the outer cylinder can be established by considering the forces acting on a cylinder element shown in Figure 4.1. Thereby we need to consider force components in the direction $\varphi = 0$ only, because the other components cancel each other due to the circular symmetry assumed.

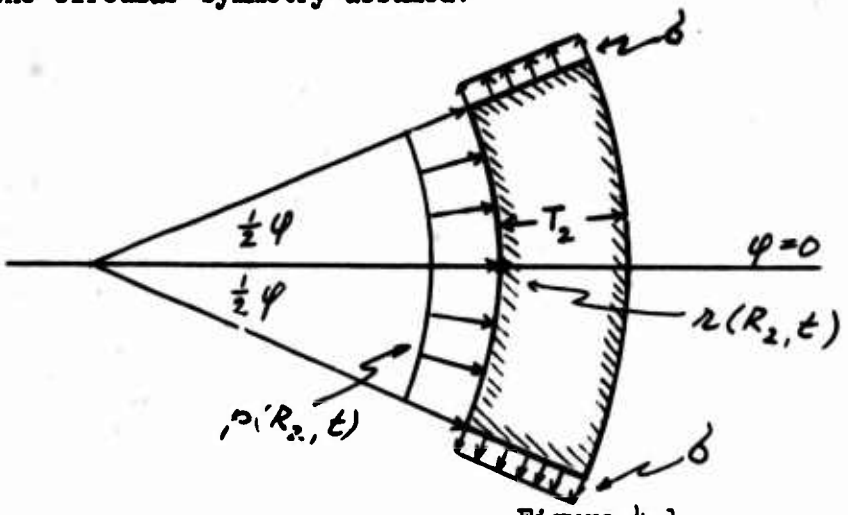

Figure 4.1

The resultant of the pressure in the direction $\varphi = 0$ is

$$F_1 = p(R_2,t)\cdot r(R_2,t)\cdot h\cdot 2 \sin \frac{1}{2}\varphi, \qquad (4.1)$$

where h is the height of the cylinder element.

About the stresses within the metal we assume that they can be approximated by an average value σ across the thickness T_2. Assuming a linear elasticity law with the modulus of elasticity E we obtain then the following expression for the force component F_2 resulting from stresses:

$$F_2 = - \sigma T_2 h \, 2 \sin \frac{1}{2} \varphi = \\ = - E \frac{r(R_2,t) - R_2}{R_2} \cdot T_2 \cdot h \cdot 2 \sin \frac{1}{2} \varphi. \tag{4.2}$$

The mass of the cylinder element is

$$M = \rho_2 R_2 T_2 \, h \, \varphi + \rho_2 \frac{1}{2} T_2^2 \, h \, \varphi \tag{4.3}$$

where ρ_2 is the density of the cylinder material.

Equilibrium of forces acting on the cylinder element furnish the equation

$$\rho_2 R_2 T_2 (1 + \frac{T_2}{2R_2}) \frac{\partial^2 r}{\partial t^2} = (pr - E \frac{r-R_2}{R_2} T_2) \frac{2 \sin \frac{1}{2} \varphi}{\varphi} . \tag{4.4}$$

For $\varphi \to 0$ we obtain

$$\frac{\partial^2 r}{\partial t^2} = \frac{r(R_2,t) \; p \; (R_2,t)}{\rho_2 T_2 R_2 (1 + T_2/2R_2)} - \frac{E}{\rho_2 R_2} \cdot \frac{r(R_2,t) - R_2}{R_2 (1 + T_2/2R_2)} . \tag{4.5}$$

The pressure $p(R_2,t)$ can be expressed in an adiabatic flow with (2.11) by

$$p(R_2,t) = p(R_2,0) \left(\frac{R_2}{r(R_2,t) \cdot \partial r(R_2,t)/\partial R} \right)^{\gamma} . \tag{4.6}$$

Substitution of (4.6) into (4.5) yields then the boundary condition for $R = R_2$. Expressed in terms of the variables x and u(x,t) this boundary condition is

$$u_{tt}(b,t) = P(b)\frac{\rho(b,0)}{\rho_2 W_2} \cdot \left(\frac{b}{u}\right)^{\gamma-1} \frac{1}{u_x^{\gamma}} - \frac{E}{\rho_2 b} \cdot \frac{u-b}{b} \cdot \frac{T_2}{W_2}, \tag{4.7}$$

where $P(x) = p(x,0)/\rho(x,0)$ is a parameter of the differential equation (see (2.18)) and W_2 is defined by

$$W_2 = T_2\left(1 + \frac{T_2}{2R_2}\right). \tag{4.8}$$

The quantity W_2 has the dimension of a length and it characterizes together with ρ_2 the casing. Normally $T_2 << R_2$ and consequently, $W_2 \approx T_2$, i.e., W_2 is approximately equal to the thickness of the casing.

The boundary condition (4.7) is of the form

$$u_{tt}(b,t) = F_M - F_S, \tag{4.9}$$

i.e., the acceleration of the casing is proportional to the difference between a term F_M which depends on the mass of the casing and a term F_S which depends on the strength of the casing.

F_S has the form indicated in (4.7) during the first phase of the movement only. Once the yield stress σ_y in the cylinder is surpassed, the linear stress-strain law ought to be replaced by a different assumption. Assuming for instance a constant stress in the cylinder for the phase between the yield point and rupture point we obtain for F_S the approximation

$$F_S = \begin{cases} \frac{E}{\rho_2 b} \cdot \frac{u(b,t) - b}{b} \cdot \frac{T_2}{W_2}, & \text{if} \quad u < b(1 + \sigma_y/E) \\ \frac{E}{\rho_2 b} \cdot \frac{\sigma_y}{E} \cdot \frac{T_2}{W_2} & \text{if} \quad b(1 + \sigma_y/E) \leq u < b(1 + \epsilon_r) \\ 0, & \text{if} \quad b(1 + \epsilon_r) \leq u. \end{cases} \tag{4.10}$$

The quantity ϵ_r in (4.10) is the deformation of the cylinder at the rupture point. Experiments have indicated that for steel cylinders[3,8] $\epsilon_r \approx 0.2 - 0.6$. The formula (4.10) for F_S may be replaced by a more complicated formula if a contraction of the casing during the movement is possible. Generally in such cases a hysteresis in the stress-strain law must be taken into account. The inclusion of such conditions in (4.7) is straightforward and most easily done at the level of numerical calculations.

At the beginning of the motion $F_S = 0$ and F_M is large. As $u(x_2,t)$ increases, F_S increases too, whereas F_M decreases. In all technically interesting cases, however, F_M is at the rupture point still larger than F_S by several orders. Therefore, the term F_3 might be dropped in (4.7) altogether. On the other hand, its inclusion into the boundary conditions is straightforward and may be done anyhow, especially if the computations are done by fixed machine codes. Its inclusion in such codes will save the user from the necessity to check the significance of F_S in any particular case. The parameters E, σ_y and ϵ_r of F_S are normally known more accurate than the parameter P(b) in the term F_M.

The first term F_M in the boundary condition (4.9) represents the action of the pressure of gas on the inner surface of the casing. After rupture of the cylinder the gas may escape freely through the gaps and it has been suggested that no further acceleration of the cylinder fragments takes place[3]. The latter assumption will probably underestimate the fragment velocity. In order to obtain an upper bound for that velocity, we may assume that the fragments retain their shape after fragmentation and are accelerated by a force proportional to the gas pressure times the

surface area of the fragments. With this assumption we obtain for F_M the formula

$$F_M = P(b)\,\frac{\rho(b,0)}{\rho_2 W_2}\,\left(\frac{b}{u}\right)^{\gamma-1}\,\frac{1}{u_x^{\gamma}}\cdot \min\left(1,\frac{x_r(1+\varepsilon_r)}{u(b,t)}\right). \qquad (4.11)$$

In case the cylinders are degenerated into plates, no considerations about the strength of the material are necessary. The right side of the boundary condition (4.9) is then given simply by

$$F_M = P(b)\,\frac{\rho(b,0)}{\rho_2 T_2}\cdot u_x(b,t)^{-\gamma}$$
$$F_S = 0 \qquad (4.12)$$

Note, that in this case the product $\rho_2 T_2$ enters the boundary conditions instead of $\rho_2 W_2$.

CHAPTER 5
BOUNDARY CONDITIONS FOR THE LINER

Boundary conditions for the gas flow at the inner cylinder ("liner") can be established by considerations similar to those of Chapter 4. Let the density of the cylinder material be ρ_1 and the initial thickness of the cylinder be T_1. The outer initial radius of the liner is R_1. As boundary conditions during a first phase of the motion we obtain then an equation of the same type as (4.9), namely

$$u_{tt}(a,t) = f_M - f_S. \qquad (5.1)$$

The first term on the right hand side of (5.1) represents the action of the pressure and it depends on the mass of the cylinder:

$$f_M = -\,P(a)\,\frac{\rho(a,0)}{\rho_1 W_1}\,\left(\frac{a}{u}\right)^{\gamma-1}\,\frac{1}{u_x^{\gamma}}\,, \qquad (5.2)$$

with

$$w_1 = T_1\left(1 - \frac{T_1}{2R_1}\right) . \tag{5.3}$$

w_1 is a parameter of the liner, approximately equal to its thickness. P(x) is the parameter of the differential equation defined by (2.18).

The more interesting and problematic second term in (5.1), f_S, which depends on the strength of the material will be discussed further below.

If the explosion is sufficiently strong to cause the liner to collapse, then eventually it will be compressed into a solid cylinder which we assume is rigid. Consequently the boundary condition changes into

$$u(a,t) \equiv u_{min} = \text{const.} \tag{5.4}$$

after this stage is reached. The value of u_{min} is

$$u_{min} = \sqrt{\frac{\rho_1}{\rho_{1\ max}}\ 2\ w_1 R_1} , \tag{5.5}$$

where $\rho_{1\ max}$ is the density of the liner after total compression. Normally for metal cylinders one would assume $\rho_{1\ max} = \rho_1$.

The complete boundary conditions are then

$$\begin{aligned} u_{tt}(a,t) &= f_M - f_S \quad \text{for} \quad u(a,t) > u_{min}, \\ u_t(a,t) &\equiv 0 \qquad\quad \text{for} \quad u(a,t) = u_{min}. \end{aligned} \tag{5.6}$$

The term f_S in (5.6) can be computed for the beginning of the motion by assuming a linear stress-strain law. We obtain thus for the elastic phase

$$f_S = \frac{E}{\rho_1 a} \cdot \frac{u(a,t) - a}{a} \cdot \frac{T_1}{w_1} \quad \text{if} \quad a(1 - \sigma_y/E) < u(a,t) \leq a \tag{5.7}$$

where E is the modulus of elasticity of the liner and σ_y is its yield stress.

Little is known about the behavior of the liner if after the yield point is surpassed further compression takes place. Obviously the liner will be buckled or even damaged during this phase. Fragments of material will be driven toward the axis of the cylinder and pushed into a wedge. They may be pressed together into a new layer immediately after fragmentation adding thus to the strength of the cylinder. It is as easy to give plausible reasons for an increase of f_S as for a decrease of f_S during this phase. As a working hypothesis we may, therefore, assume that f_S = const. after the yield point is surpassed. The complete formula for f_S is then

$$f_S = \begin{cases} \dfrac{E}{\rho_1 a} \cdot \dfrac{u(a,t) - a}{a} \cdot \dfrac{T_1}{w_1} & \text{if } a(1 - \sigma_y/E) < u(a,t) \leq a \\ \dfrac{E}{\rho_1 a} \cdot \dfrac{\sigma_y}{E} \cdot \dfrac{T_1}{w_1} & \text{if } u_{min} < u(a,t) \leq a(1 - \sigma_y/E) \end{cases} \tag{5.8}$$

As for the casing, we can easily include a hysteresis type stress-strain relation in the formula for f_S if expansion of the liner during the motion takes place.

The hypothesis about f_S can be checked by measuring the liner velocity in experiments. The function $f_S(u(a,t))$ can then be modified to fit the experimental results. An indirect testing of the working hypothesis is possible, too. We may assume that the work required for the

deformation of the liner is transformed into heat. The compressed liner should have, therefore, a high temperature after the explosion. (Heating of the liner by heat conduction should be negligible because of the short duration of the process. The compression is completed within some 10^{-5} seconds[3].) The heat contents of the liner can be measured and compared with the theoretical value according to the working hypothesis. With the assumption (5.8) the work against the stresses becomes

$$W = \pi\, h\, T_1\, R_1\, \sigma_y \left\{\frac{\sigma_y}{E} + \frac{2}{R_1}\,(u_{yield} - u_{min})\right\}, \qquad (5.9)$$

where u_{yield} is the radius of the liner at the yield point and h is the height of the cylinder. The first term in the braces in (5.9) represents the contribution to the work during the elastic phase of compression and the second term is the contribution due to the working hypothesis.

The temperature increase of the liner due to W is

$$\tau = \frac{W}{M_1 c_m}\,, \qquad (5.10)$$

where M_1 is the mass of the liner and c_m is its specific heat. Substituting (5.9) into (5.10) we obtain for the temperature increase

$$\tau = \frac{\sigma_y T_1}{c_m \rho_1 w_1} \left\{\frac{\sigma_y}{E} + \frac{2}{R_1}(u_{yield} - u_{min})\right\}. \qquad (5.11)$$

In case the liner is degenerated into a plate the boundary condition becomes particularly simple. In this case we have

$$f_M = -\,P(a)\frac{\rho(a,0)}{\rho_1 T_1} \cdot u_x(a,t)^{-\gamma}\,, \qquad (5.12)$$
$$f_S \equiv 0.$$

CHAPTER 6
INITIAL CONDITIONS

We obtain simple initial conditions for the problem if we assume that a constant volume detonation has turned the explosive into gas completely some time before the cylinders start moving. We can then assume that the pressure and density are constant throughout the gas and that the gas is at rest. The parameters of the differential equation (see (2.18)) become

$$P(x) = \frac{p(x,0)}{\rho(x,0)} \equiv P_o = \text{const.},$$
$$Q(x) = \frac{p_x(x,0)}{p(x,0)} \equiv 0. \tag{6.1}$$

and the initial values for $u(x,t)$ are

$$u(x,0) = x$$
$$u_t(x,0) \equiv 0 \tag{6.2}$$

The numerical value of P_o is easily obtained from the energy E_o per mass unit of the explosive. After the constant volume detonation the whole energy released is transformed into heat. Since we have assumed that the explosive fumes are a perfect gas we obtain the equation (Ref. 1,p. 9)

$$E_o = \frac{1}{\gamma-1} \frac{p(x,0)}{\rho(x,0)} = \frac{1}{\gamma - 1} P_o \tag{6.3}$$

or

$$P_o = (\gamma-1) \cdot E_o. \tag{6.4}$$

The values of E_o and γ are known quantities for a given explosive. For example, for pentolite we have the values[4]

$$E = 1.152\ [\text{kcal/g}] = 4.822 \cdot 10^{6}\ [\text{m}^2/\text{sec}^2],$$
$$\gamma = 3.2,$$
$$P_o = 1.06 \cdot 10^{7}\ [\text{m}^2/\text{sec}^2].$$

If the space between the cylinders is filled only partly with explosive, the initial value $\rho(x,0)$ will be a fraction of the explosive's density. However, the pressure $p(x,0)$ is reduced correspondingly in such cases and the parameter P_o remains unchanged. Hence this parameter is a characteristic property of the explosive, independent of the particular loading, as demonstrated by (6.4).

The loading density $\rho(x,0)$ enters the boundary conditions only, as shown by (4.11) and (5.2).

The assumption of a constant pressure and density throughout the gas at the beginning of the process is certainly a quite rough approximation to the reality. On the other hand it is virtually impossible to furnish such non-constant generally valid initial conditions which may be justified by the setup of experiments. The initiation of the detonation is in a real case invariably done at one or both ends of the cylinder and, therefore, the real problem is not one-dimensional anyhow. A constant initial status seems not to be a more serious idealization than the other assumptions outlined in Chapter 1. The final justification of the idealizations is, of course, the experiment. If the numerical results obtained by solving the differential Equations (2.16) or (2.17) do not agree within reasonable errors with experiments, we have to reconsider all idealizations.

CHAPTER 7
NUMERICAL SOLUTION

The technical problem outlined in Chapter 1 was formulated in Chapter 2 as a quasi-linear second order partial differential equation. The initial and boundary conditions for the equation were derived in Chapters 4, 5 and 6. For the numerical solution of this equation we will propose in this Chapter a two-level difference scheme. Such a scheme uses data at $t = t_k$ only to compute the solution at $t_{k+1} = t_k + l_{k+1}$. Usually, for second order problems difference schemes with more levels are used. The reasons for applying a two-level scheme on the present problem are as follows:

(1) A two-level scheme permits a simple change of the size of the time step l_{k+1}, depending on computed results. This property is of great practical value if dealing with non-linear equations.

(2) The solution by the two-level scheme presented in this Chapter furnishes concurrently with $u(x,t)$ also $u_t(x,t)$. Since for the present problem the values of u_t at boundaries are of principal interest, the scheme meets practical needs by avoiding a numerical differentiation of the results.

The difference scheme will be described only briefly in this Chapter. A detailed analysis of the scheme will be published in a forthcoming paper.

The difference scheme is applied to a rectangular grid in the x,t-plane defined by

$$x_i = x_o + ih \quad , \quad (i = 0,1,2,\ldots,n),$$

$$t_k = t_o + \sum_{j=0}^{k} l_j \quad , \quad (k = 0,1,2,\ldots; l_o = 0), \tag{7.1}$$

(see Figure 7.1). The correct values of $u(x,t)$ at the grid points we denote by

$$u_{i,k} = u(x_i, t_k)$$

and approximations to $u_{i,k}$ by $U_{i,k}$.

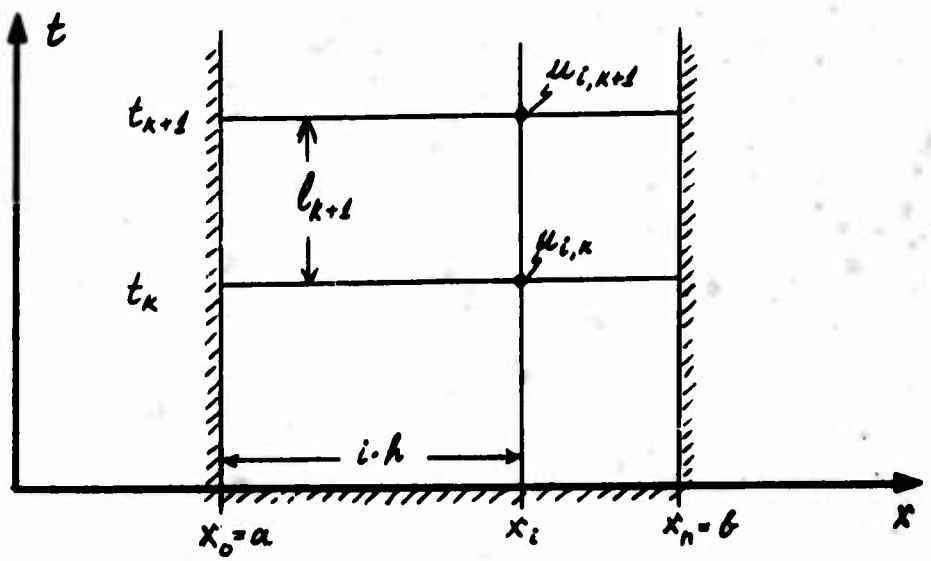

Figure 7.1.

In order to reduce the number of indices, we will denote in the sequel the partial derivatives $\partial/\partial t$ by dots and the partial derivatives $\partial/\partial x$ by apostrophes.

The basis for the difference scheme are the relations

$$u_{i,k+1} = u_{i,k} + l_{k+1}\,\dot{u}_{i,k} + \frac{1}{3}\,l_{k+1}^2\,\ddot{u}_{i,k} + \frac{1}{6}\,l_{k+1}^2\,\ddot{u}_{i,k+1} + R_1 \tag{7.2}$$

with

$$R_1 = - u^{4\cdot}(x_i, t_k + \theta_1 l_{k+1}) \frac{l_{k+1}^4}{24}, \quad (0 \le \theta_1 \le 1) \tag{7.3}$$

and

$$\dot{u}_{i,k+1} = \dot{u}_{i,k} + \frac{1}{2} l_{k+1} \ddot{u}_{i,k} + \frac{1}{2} l_{k+1} \ddot{u}_{i,k+1} + R_2 \tag{7.4}$$

with

$$R_2 = - u^{4\cdot}(x_i, t_k + \theta_2 l_{k+1}) \frac{l_{k+1}^3}{12}, \quad (0 \le \theta_2 \le 1). \tag{7.5}$$

For the approximate solution we drop the remainder terms R_1 and R_2 in (7.2) and (7.4), respectively. In order to compute U and $\dot{U}$ at grid points with $t = t_{k+1}$ by the truncated formulae we need then the values of U, $\dot{U}$ and $\ddot{U}$ at $t = t_k$ and $\ddot{U}$ at $t = t_{k+1}$. The first two quantities are known for the first time step from initial conditions. Proceeding with the computations by one time step at a time we have these values available for $t = t_k$ when computation of U and $\dot{U}$ for $t = t_{k+1}$, starts. The value of $\ddot{U}$ we obtain by using the differential equation

$$\ddot{U} = d(x,t,U,\dot{U},U') \; U'' + e(x,t,U,\dot{U},U'). \tag{7.6}$$

The values of the arguments x, t, U and $\dot{U}$ of d and e are known for $t = t_k$. The values of U' and U'' are computed by numerical differentiation of U. The necessary formulae follow from the relations

$$u'_{i,k} = \frac{1}{2h} (u_{i+1,k} - u_{i-1,k}) + S_1 \tag{7.7}$$

with

$$S_1 = - u'''(x_i + \theta_3 h, t_k) \frac{h^2}{6}, \quad (-1 \le \theta_3 \le 1) \tag{7.8}$$

and

$$u''_{i,k} = \frac{1}{h^2} (u_{i+1,k} - 2u_{i,k} + u_{i-1,k}) + S_2 \tag{7.9}$$

with

$$S_2 = - u^{IV}(x_i + \theta_4 h, t_k) \cdot \frac{h^2}{12}, \quad (-1 \le \theta_4 \le 1). \tag{7.10}$$

For the numerical differentiation of U we drop S_1 and S_2 in (7.8) and (7.10), respectively.

The last quantity needed in (7.2) and (7.4) is $\ddot{U}_{i,k+1}$. It is approximated as follows:

First we compute

$$*U_{i,k+1} = U_{i,k} + l_{k+1} \dot{U}_{i,k} + \frac{1}{2} l_{k+1}^2 \ddot{U}_{i,k}, \tag{7.11}$$

$$*\dot{U}_{i,k+1} = \dot{U}_{i,k} + l_{k+1} \ddot{U}_{i,k}, \tag{7.12}$$

$$*U'_{i,k+1} = \frac{1}{2h} (*U_{i+1,k+1} - *U_{i-1,k+1}), \tag{7.13}$$

$$*U''_{i,k+1} = \frac{1}{h^2} (*U_{i+1,\,k+1} - 2*U_{i,k+1} + *U_{i-1,k+1}). \tag{7.14}$$

Using these values and the differential Equation (7.6) with $t = t_{k+1}$, we obtain then a value $*\ddot{U}_{i,k+1}$. This value we use as approximation of $\ddot{u}_{i,k+1}$ in (7.2) and (7.4).

By this all terms on the right hand of (7.2) and (7.4) are estimated (except for the remainder terms R_1 and R_2 which are dropped). The trunctated formulae (7.2) and (7.4) thus furnish the values of $U_{i,k+1}$ and $\dot{U}_{i,k+1}$ and the computing process starts anew with $k + 1 = k$.

It can be shown that the approximations obtained by this computing scheme have the following error orders if $u_{i,k}$ and $\dot{u}_{i,k}$ are known exactly and certain higher order derivatives of u are bounded:

Error order of $U_{i,k+1}$: $\quad O(l_{k+1}^4) + O(l_{k+1}^2 h^2)$,

Error order of $\dot{U}_{i,k+1}$: $\quad O(l_{k+1}^3) + O(l_{k+1} h^2)$.

We note that these error orders are the same if the computational scheme is applied to the more general non-linear differential equation $\ddot{u} = f(x,t,u,\dot{u},u',u'')$.

The flexibility of the scheme with respect to changes of the time interval l can be exploited by choosing at every time step a different interval in accordance with some criterion. A reasonable choice from the view point of the physical phenomena involved is to select l_{k+1} such that the domain of dependence for the point x_i, t_{k+1} is for $t = t_k$ within the interval $x_{i-1} \leq x \leq x_{i+1}$ (Ref. 5, p. 275). Because the domain of dependence can depend on x we chose for l_{k+1} the corresponding minimum over all x_i:

$$l_{k+1} = h \cdot \min_{i=1,\ldots,n-1} \left\{ \left(d(x_i, t_{k,\ldots}) \right)^{-1/2} \right\} . \qquad (7.15)$$

An investigation of the stability of the scheme (in the sense of Richtmyer[6]) shows that the amplification matrix satisfies the necessary von Neumann stability condition if

$$l_{k+1} \leq h \frac{\sqrt{3}}{\sqrt{d(x,t_{k,\ldots})}} \qquad (7.16)$$

Hence, by chosing l_{k+1} in accordance with (7.15) we remain well apart from the von Neumann instability bound.

CHAPTER 8
TESTS OF THE SOLUTION

In order to test the feasibility of the idealizations assumed and of the numerical solution process used, some gas flows were computed and compared with experiments and asymptotic formulae.

The only experimental data available were contained in a report about fragment velocities obtained from positions of fragments of the casing at different time intervals after explosion[7]. Unfortunately this report does not give the particular positions observed but gives certain averages and average velocities instead. Therefore, these data can be used to compare the orders and trends of the fragment velocities only.

A description of the cylinders exploded in the experiments is given in Table I. The fragment positions for Experiments 2 and 3 and the corresponding results of computations are shown in Figure 8.1.

The computed values $u(b,t)$ are in both examples plotted in Figure 8.1 higher than those of the experiments, except for the first parts of the curves. Such a general behavior is to be expected because the computation does not take into account the finite lengths of the cylinders which permit the gas to escape through the ends of the cylinders. Moreover, the fragment positions plotted are obtained by averaging the positions of fragments from ends of the cylinder and from the central zone of the cylinder. For the present purpose a comparison with the higher values from the central zone would be more reasonable. A third effect of unknown magnitude is the effect of the surrounding air on the fragment positions.

Table I. Parameters of Experiments

Experiment Number	Liner			Casing			Loading Density	Height of Cylinder
	R_1	T_1	ρ_1	R_2	T_2	ρ_2	ρ_o	h
1	1.905	0.124	2.77	4.246	0.199	7.8	0.406	4.762
2	3.490	-	∞	4.246	0.199	7.8	0.999	9.525
3	0	-	∞	1.562	0.343	7.8	1.646	10.952

The radii $R_{1,2}$ and thicknesses $T_{1,2}$ are given in centimeters.

The densities $\rho_{0,1,2}$ are given in g/cm^3. (Infinite ρ_1 means rigid liner.)

The strengths of the casing and lining were found negligible in the cases considered. They were not included in the computations.

For the characterization of the charge the values of pentolite[4] were used:

Energy per unit mass $E_o = 4.82.10^6\ m^2/sec^2$

Ratio of specific heats $\gamma = 3.2$

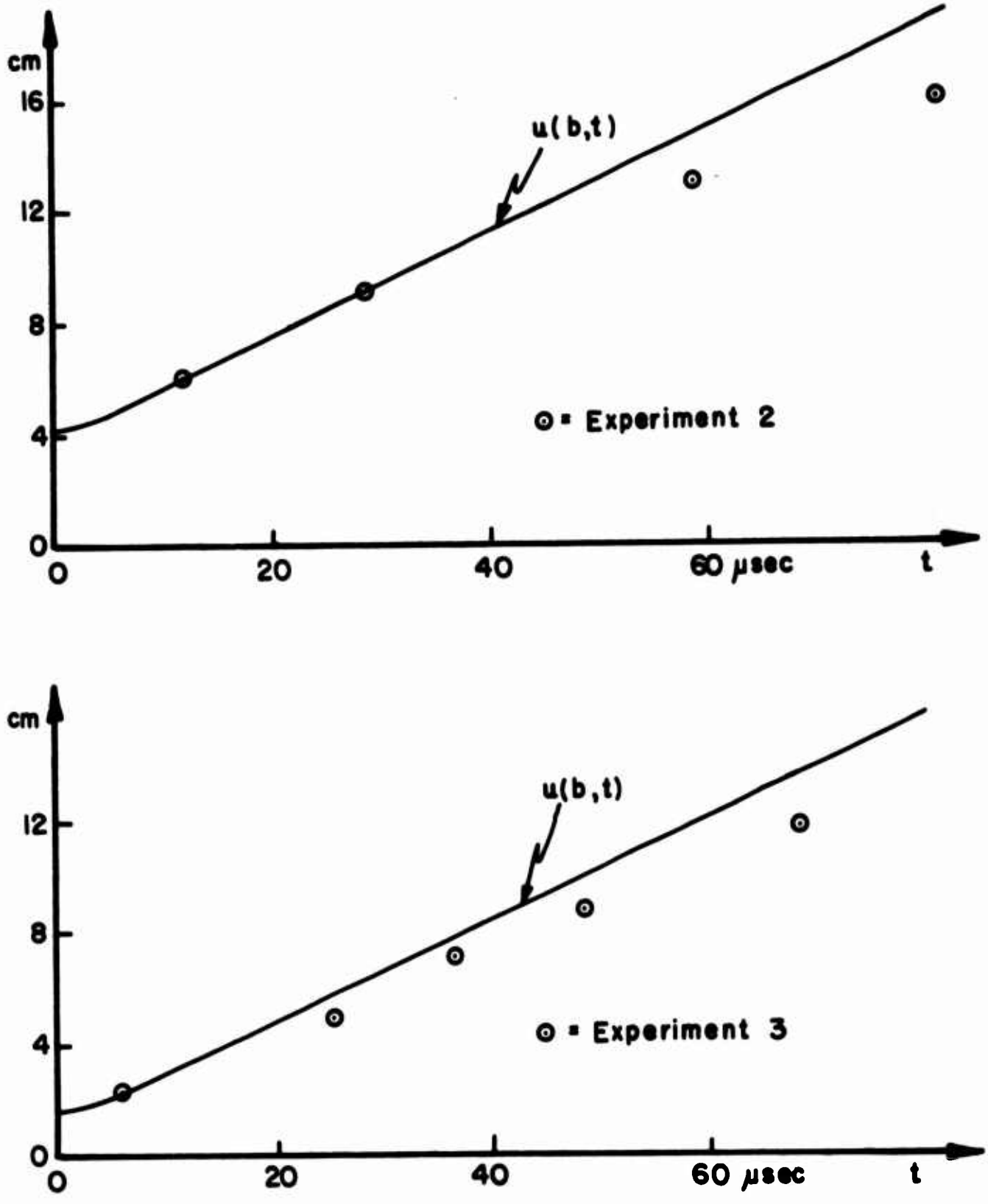

Figure 8.1. Positions of casing

The report about the experiments does not give fragment positions for Experiment 1 where two hollow cylinders were involved. Averages of the ratios $\bar{v}$ = (distance flown by fragments)/(flight time) for various zones are reported instead. These values are compared with the computations in Table II. The larger discrepancy between observed and computed values for long flight times is certainly to a great extent due to the fact that the exploded cylinder's diameter is almost twice as large as its height. Therefore, a close agreement with the behavior of an infinite long cylinder cannot be expected. Note also the large variation of average $\bar{v}$ - values in the experiment.

In all three experiments a closer agreement with computed values is obtained for short times after the explosion. The agreement becomes less good with increased time as unknown factors influence the fragment velocities. Since the main objective of the computations is the study of the behavior of the cylinders during very short times after the explosion (i.e., during the collapse of the liner), the comparison with experiments can be considered as satisfactory.

For Experiments 2 and 3 the fragment velocities can be computed also by approximate formulae derived by Gurney and Sterne and quoted in the appendix. These formulae are derived under the assumptions that the inner cylinder is rigid, the density of the gas is constant and the gradient of the particle velocity of the gas is constant, too. With these assumptions the velocity of the outer cylinder (i.e., fragments) can be computed equalizing the kinetical energy of the system with the energy contained in the explosive. Since the assumptions of constant density

Table II. Comparison of Experiment 1 with Computations

EXPERIMENT 1

Zone height [cm]	Average $\bar{v}$[m/sec]
2.76	538
2.38	1058
2.00	1044

The total height of the cylinders were 4.76 cm. The averages $\bar{v}$ were obtained by averaging results of a number of experiments for three different zones of the cylinders, specified by their respective heights.

COMPUTATION

$\bar{v}$[m/sec]	v[m/sec]	Time
652	1090	At t = 6.4 μ sec; collapse time of the liner.
846	1243	At t_r = 10.1 μ sec; estimated rupture time of the casing, i.e., $u(b,t_r) = 1.2 \cdot b$.
1462	1580	At t = 100 μ sec. Further increase of v is insignificant.

$v = \dot{u}(b,t)$ = fragment velocity

$\bar{v} = (u(b,t) - b)/t$ = (distance flown by fragments)/(flight time)

and constant velocity gradient are certainly most closely satisfied after considerable expansion of the cylinders, the velocities computed with Sterne's formulae can be considered as approximations to the asymptotic values of the fragment velocities. A comparison of Sterne's values with those obtained by the solution of the differential equation can be considered, therefore, as a check of the numerical integration process. The values obtained are compared in Table III. The close agreement between these values excludes the numerical integration as a reason for differences between experiments and calculations for large t. These differences are, therefore, caused by the idealizations of the problem.

Some typical results of the calculations are shown in Figures 8.2, 8.3 and 8.4. The Figure 8.2 shows some pressure profiles of the gas flow corresponding to Experiment 1 at various instants. It is interesting to note that the pressure increases within the centripetal flow near the axis already before the liner is compressed into a solid cylinder. Such a behavior of the flow was anticipated in Chapter 3. After the compression of the liner the flow is reflected at the now rigid inner cylinder and a high pressure wave proceeds into the gas. The pressure decays rapidly with increasing radius because of the geometry of the flow. At the time the wave reaches the casing the pressure has dropped below 2000 atmospheres in this example.

The Figure 8.3, upper part, shows the positions of the liner and of the casing of Experiment 1 as functions of time. It permits, however, the following different interpretation. Assume that the detonation was initiated at the right hand end of a cylinder and that it proceeds with

Table III. Comparison of Asymptotic Formulae with Results of Integration

Experiment Number	Fragment Velocities [m/sec]	
	Asymptotic Value	Result of Integration
2	1865 for $u_{rupt} = 1.6 \cdot R_2$ 1900 for $u_{rupt} = 1.2 \cdot R_2$	1878 at t = 113 μ sec
3	1852	1845 at t = 170 μ sec
Sandwich	V_A = 1335 V_B = 3308	V_A = 1336 V_B = 3308 at t = 104 μ sec

The thicknesses and densities of the plates in the "Sandwich" case were assumed equal to the thicknesses and densities of the cylinders in Experiment 1.

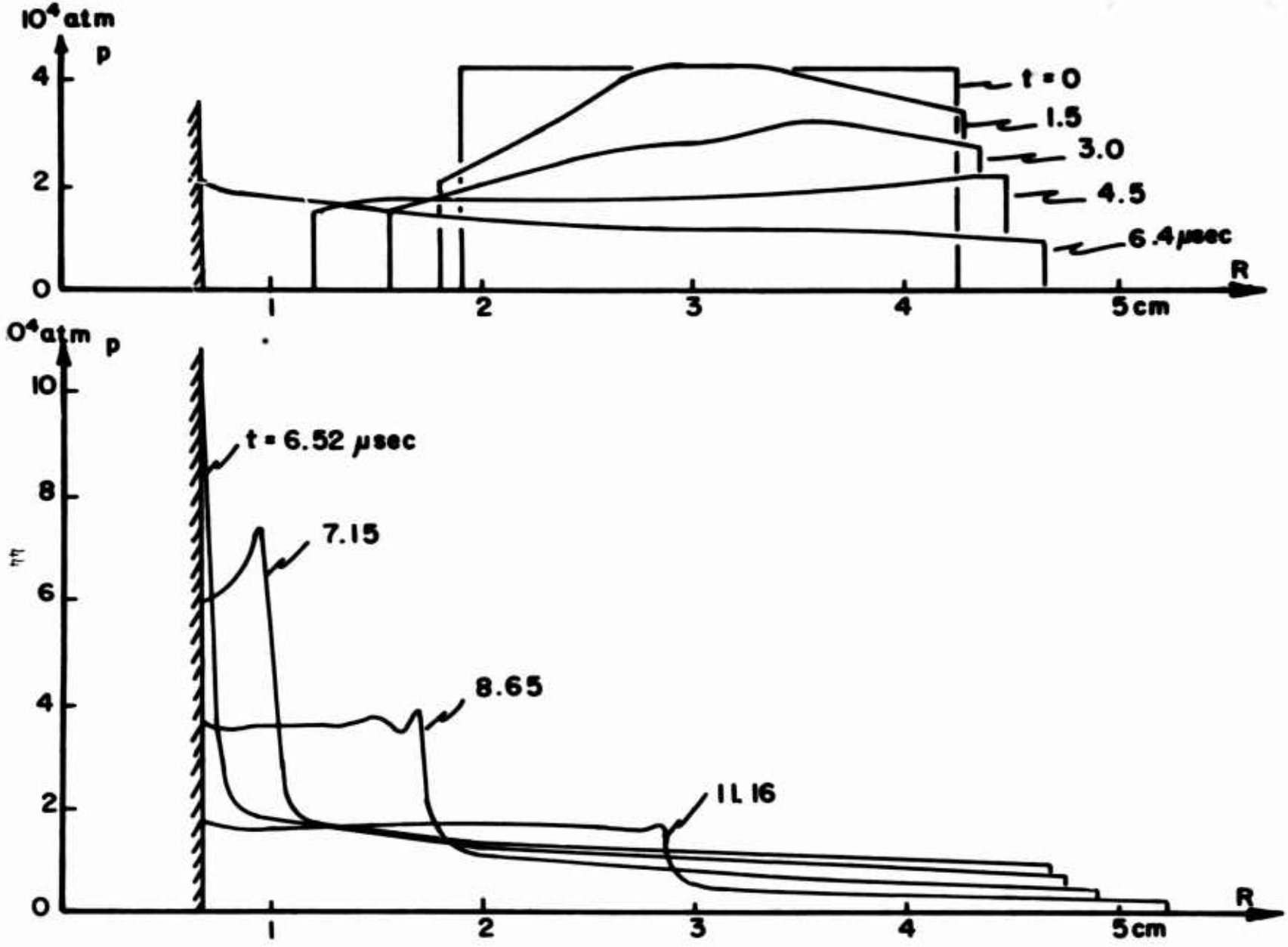

Figure 8.2 Pressure profiles

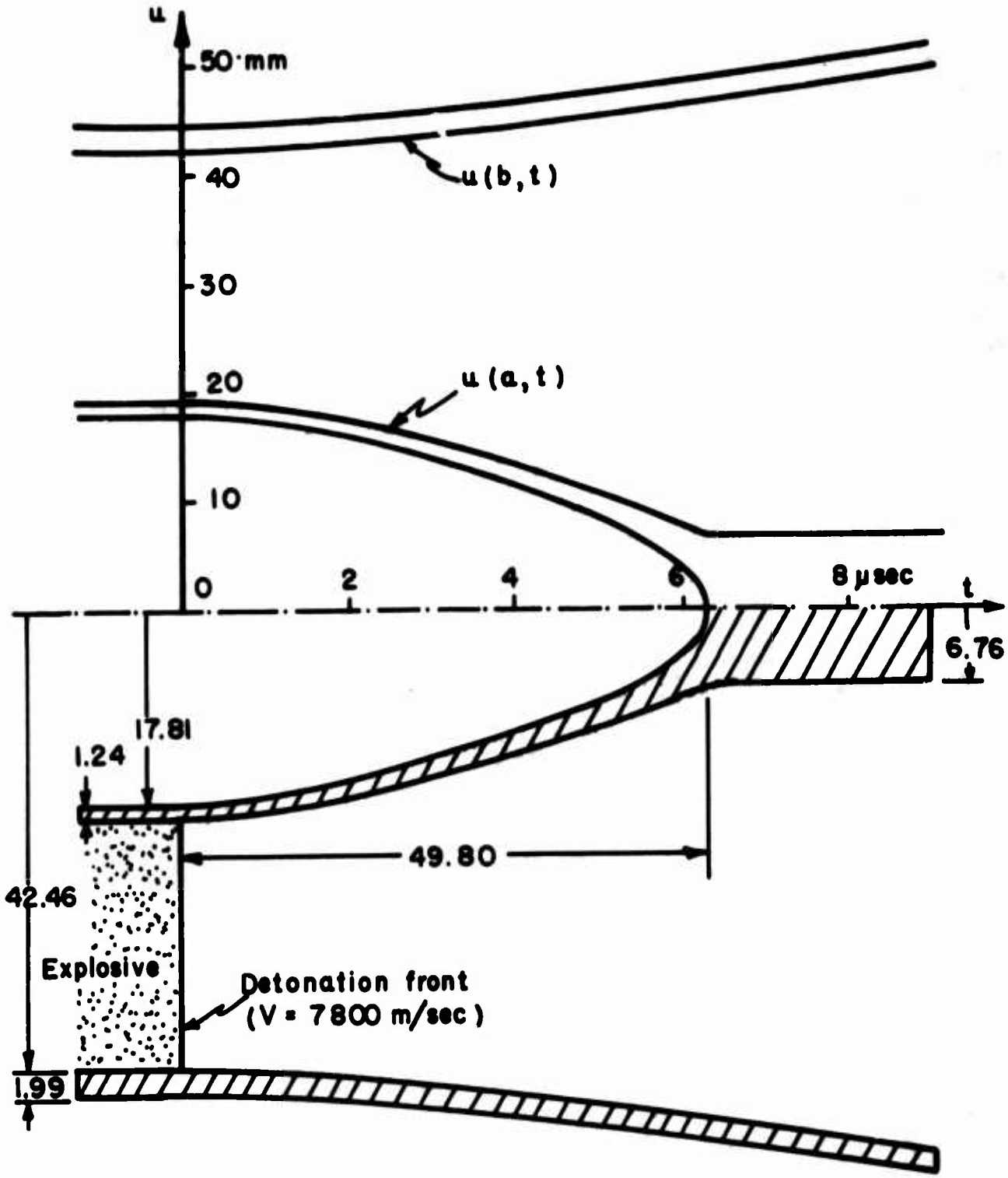

Figure 8.3. Collapse profile

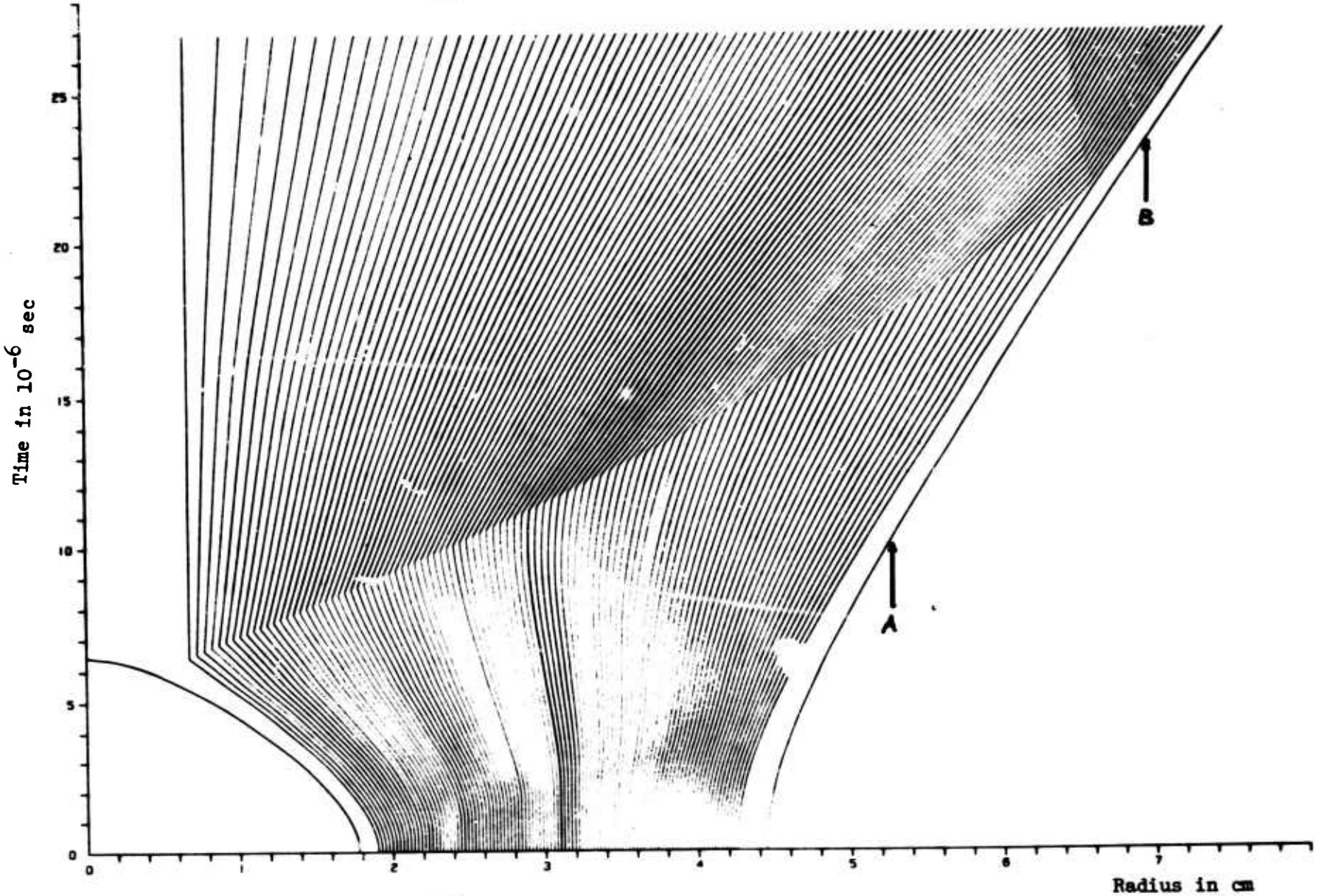

Figure 8.4. Particle paths

a constant speed to the left. We may consider the Figure 8.3 then as a picture of the partly damaged cylinder at a fixed time. The lower part of the Figure shows such an interpretation with the assumption that the velocity of the detonation front is 7800 m/sec. It would be highly interesting and instructive to compare the computed collapse profile of the liner with experimental data.

Figure 8.4 is identical to the upper part of Figure 8.3 with the paths of gas particles included. The form of these paths suggests the presence of a shock caused by reflection of the gas flow at the rigidly compressed liner. Since this shock develops only after the liner is completely compressed it does not influence the behavior of the liner during collapse. From a practical view point there is, therefore, no need to employ a more sophisticated computing process which permits to consider entropy changes caused by the shock.

In the present case, however, the computations were carried on after the development of the shock in order to obtain data which could be compared with experiments. A discussion of the effects of the neglected entropy changes on these data is therefore in place.

The most striking behavior of the high pressure wave in Figure 8.1 is its rapid decay which is caused by the geometry of the flow. At the time the wave reaches the casing the pressure has dropped to a small fraction of the initial pressure. Since the geometry affects a shock in a similar manner we can expect that an outward moving shock will also rapidly decay. A small shock can be replaced for computational purposes by a wave[1]. Therefore, the difference between shock and wave

calculations becomes smaller with increasing time and distance from the axis. The magnitude of the pressure in the wave is such that its influence on the casing is negligible in the example computed. In this example which is typical for the applications we have moreover other more serious effects on the behavior of the casing neglected, namely the effect of the fragmentation. The fragmentation of the casing takes place somewhere between the points A and B in Figure 8.4. The shock (or wave) reaches the casing after or immediately before fragmentation. The position of the casing before fragmentation is, therefore, not influenced by the reflected shock. Any comparison with experiments should be made during this phase. Once the casing is fragmented the agreement between computed and measured positions is likely to become bad, whatever the accuracy of the computation of the flow. The computation of a shock would influence the results (position of the casing) only for this phase. Hence even for large time values (as in the present case) the possible merits of a consideration of the shock are questionable.

In order to test the computations for cylinders which are degenerated into plates the computational results were compared with Sterne's formulae for sandwich flows. Experimental data for such flows were not available. For the plates the thicknesses and densities of the cylinders of Experiment 1 were assumed and also the same loading density was used. The resulting velocities are listed in Table III and they agree perfectly with Sterne's values.

CHAPTER 9
CONCLUSIONS

The computation of hollow cylinder explosions by the process outlined in this paper furnish reasonable results in spite of the coarse idealizations assumed. The fair agreement of computed results with experiments indicates that a refined theory lacks a testing basis at the present time. Therefore, a more sophisticated theoretical treatment of the problem may be delayed until more precise and more detailed experimental results are made available. In Chapters 5 and 8 some special experiments are proposed for this purpose.

The method presented provides simple means to compute fragment and collapse velocities for long co-axial cylinders. The accuracy of the computations cannot be checked thoroughly because corresponding experimental data are not available. Available data agree with computations for times of the order of 10 μsec after the explosion.

REFERENCES

1. R. von Mises, Mathematical Theory of Compressible Fluid Flow, Acad. Press, New York, 1958.

2. T. E. Sterne, Jour. Appl. Phys. 21 (1950), p. 73-74.

3. T. E. Sterne, A Note on the Initial Velocities of Fragments from Warheads, BRL Report No. 648, September 1947.

4. R. E. Shear, Detonation Properties of Pentolite, BRL Report No. 1159, December 1961.

5. L. Collatz, Numerische Behandlung von Differentialgleichungen, 2nd. ed. Springer, Berlin, 1955.

6. R. D. Richtmyer, Difference Methods for Initial-Value Problems, Intersc. Publ., New York, 1964.

7. H. I. Breidenbach, Fragment Velocities of Hollow Warheads as Determined from Flash Radiographs, BRL Report No. 640, June 1947.

8. I. G. Henry, The Gurney Formula and Related Approximations for the High-Explosive Deployment of Fragments, Hughes Aircraft Company, Aerospace Group, Report No. Pub-189, April 1967.

APPENDIX

STERNE'S FORMULAE

In Chapter 8 approximate formulae for the fragment velocities were used. These formulae are derived by Sterne[3]. A survey about other formulae of this type and their derivation is given by Henry[8]. Here we quote only the two Sterne's formulae used.

Case 1. Hollow Steel Cylinder with Rigid Core.

Let

E_o = energy per unit mass of the explosive,

A = ratio of outer cylinder mass by explosive's mass,

R_2 = initial radius of the outer cylinder,

R_{rup} = radius of the outer cylinder of rupture. Sterne[3] gives the value $R_{rupture} = 1.6 \cdot R_2$ whereas Henry[8] gives the value $R_{rupture} = 1.2 \cdot R_2$,

R_{core} = radius of the rigid core.

The fragment velocity is then given by

$$V_A^2 = \frac{2E_o}{A + \frac{1}{6}\frac{3R_{rup} + R_{core}}{R_{rup} + R_{core}}}$$

For $R_{core} = 0$ we obtain the corresponding formula for a cylinder filled solidly with explosive.

Case 2. Explosive between two Parallel Plates. (Sandwich Flow.)

Let

E_o = energy per unit mass of the explosive,

A = ratio of the mass of plate "A" by explosive's mass,

B = ratio of the mass of plate "B" by explosive's mass

V_A, V_B = respective velocities of the plates "A" and "B".

The velocities are given by

$$V_A^2 = \frac{6E_\phi}{(1+A+B)(1+4A+4B+12AB)}(1+2B)^2,$$

$$V_B^2 = \frac{6E_\phi}{(1+A+B)(1+4A+4B+12AB)}(1+2A)^2.$$

Unclassified
Security Classification

DOCUMENT CONTROL DATA - R & D

(Security classification of title, body of abstract and indexing annotation must be entered when the overall report is classified)

1. ORIGINATING ACTIVITY (Corporate author) U.S. Army Ballistic Research Laboratories Aberdeen Proving Ground, Maryland	2a. REPORT SECURITY CLASSIFICATION Unclassified 2b. GROUP

3. REPORT TITLE

COMPUTATION OF HOLLOW CYLINDER EXPLOSIONS

4. DESCRIPTIVE NOTES (Type of report and inclusive dates)

5. AUTHOR(S) (First name, middle initial, last name)

Aivars Celmiņš

6. REPORT DATE	7a. TOTAL NO. OF PAGES	7b. NO. OF REFS
November 1967	58	8

8a. CONTRACT OR GRANT NO.	9a. ORIGINATOR'S REPORT NUMBER(S)
b. PROJECT NO. RDT&E 1T014501A14B	Report No. 1381
c.	9b. OTHER REPORT NO(S) (Any other numbers that may be assigned this report)
d.	

10. DISTRIBUTION STATEMENT

This document has been approved for public release and sale; its distribution is unlimited.

11. SUPPLEMENTARY NOTES	12. SPONSORING MILITARY ACTIVITY
This material was presented at the 13th Conference of Army Mathematicians and will be published in the Conference Proceedings.	U.S. Army Materiel Command Washington, D.C.

13. ABSTRACT

This report treats the explosion caused by a charge which is placed between two hollow co-axial cylinders. It is assumed that at the beginning of the motion of the cylinders the explosive has been detonated completely so that the space between the cylinders is filled by a gas under high pressure. The flow of this gas during the collapse of the inner cylinder and the expansion of the outer cylinder is governed by a quasi-linear second order partial differential equation. This equation is solved numerically using a two-level difference scheme. The solution furnishes the fragment velocities of the outer cylinder and the collapse velocity of the inner cylinder. The results are compared with experimental data and asymptotic formulae.

The same computation scheme is applied to the computation of the motions of two parallel plates with a charge exploded between them. The results agree with values obtained by approximate formulae.

DD FORM 1 NOV 65 1473 REPLACES DD FORM 1473, 1 JAN 64, WHICH IS OBSOLETE FOR ARMY USE.

Unclassified
Security Classification

14. KEY WORDS	LINK A		LINK B		LINK C	
	ROLE	WT	ROLE	WT	ROLE	WT
Numerical Solution of Partial Differential Equations						
Quasi-Linear Hyperbolic Partial Differential Equation						
Cylindrical Implosion						
Collapse of a cylindrical Liner						